Systems Chemistry Hot Paper

Zitierweise: *Angew. Chem. Int. Ed.* **2023,** *62,* e202215421
Internationale Ausgabe: doi.org/10.1002/anie.202215421
Deutsche Ausgabe: doi.org/10.1002/ange.202215421

Persistent ATP-Concentration Gradients in a Hydrogel Sustained by Chemical Fuel Consumption

*Yingjuan Cao, Luca Gabrielli, Diego Frezzato, and Leonard J. Prins**

Dedicated to Professor Paolo Scrimin on the occasion of his 70th birthday.

Abstract: We show the formation of macroscopic ATP-concentrations in an agarose gel and demonstrate that these gradients can be sustained in time at the expense of the consumption of a chemical fuel. The approach relies on the spatially controlled activation of ATP-producing and ATP-consuming reactions through the local injection of enzymes in the matrix. The reaction-diffusion system is maintained in a stationary non-equilibrium state as long as chemical fuel, phosphocreatine, is present. The reaction-diffusion system is coupled to a supramolecular system composed of monolayer protected gold nanoparticles and a fluorescent probe. As a result of this coupling, fluorescence signals emerge spontaneously in response to the ATP-concentration gradients. We show that the approach permits the rational formation of complex fluorescence patterns that change over time as a function of the evolution of the ATP-concentrations present in the system.

Introduction

Life is a thermodynamically disfavored state and must be sustained by a continuous consumption of energy.[1] The non-equilibrium nature of life emerges on both the molecular and macroscopic level. Kinetic asymmetry in energy dissipation pathways drives the biomolecular machinery such as motors, transporters and pumps.[2–4] Local enzyme activity in the cell installs macroscopic concentration gradients which play an important role in regulating biological processes such as cell division and microtubule dynamics.[5,6] Inspired by the advanced functions and properties of living matter, there is a strong current interest in the development of "active" synthetic matter.[7–9] Great strides have been made in the design of artificial molecular machines that—just as in nature—are driven by chemical fuels.[10–13] On the macroscopic level, coupling of local chemical reactions with diffusion provides access to non-equilibrium phenomena such as chemotaxis, motility and pattern formation.[14–17] Such synthetic systems serve as models for understanding how dynamic concentration gradients control biological processes and would give an impetus for the development of new non-equilibrium materials.[18–20] Progress towards these objectives is facilitated by the availability of methodology that allows to rationally "sculpt" concentration gradients at the macroscopic level and maintain these gradients in time.[21–24] An attractive strategy that is emerging relies on the use of antagonistic enzymes that are activated with spatial control.[25–28] Here, we show how a macroscopic ATP-concentration gradient can be installed in a hydrogel and maintained in a (pseudo)-stationary state at the expense of chemical fuel consumption. In the hydrogel a supramolecular system consisting of interacting gold nanoparticles and fluorophores is present that dynamically responds to changes in the ATP concentration. We show that a combination of reaction kinetics, diffusion, and supramolecular processes results in the formation of macroscopic fluorescent patterns that evolve over time as a result of changes in the ATP-concentration gradient.

It is straightforward to create a concentration gradient by injecting a species in a solution without mixing, but it is not trivial to develop a stable concentration gradient between well-defined spatial positions that is sustained in time. The instalment and study of sustained ATP-concentration gradients relies on two essential features (Figure 1a). First, an ATP concentration gradient must be established and sustained at the macroscopic level through the continuous local production and consumption of ATP. Second, a molecular system is required that responds dynamically to changes in the ATP-concentration. Starting with the latter, our previous studies of multivalent complexes between AuNP **1**, which are ≈2 nm gold nanoparticles passivated with a monolayer of a C9-thiol containing a TACN·Zn^{2+} head group, and a negatively charged fluorophore, such as **A**, have shown that this system has suitable characteristics (Figure 1b).[29,30] Addition of ATP, which has a higher affinity for AuNP **1** compared to **A**, results in the displacement of **A** from the surface of AuNP **1** causing an increase in fluorescence intensity (Figure S1a). Importantly, ADP has a lower affinity for AuNP **1** and a concentration regime exists in which ATP largely displaces **A**, but ADP does so to a lower extent. We have exploited this system for the formation of transient fluorescent signals by showing that the addition of ATP to a solution containing AuNP **1**, **A** and a hydrolytic enzyme leads to the rapid displacement of **A** from AuNP **1** by ATP.[31] Upon the gradual conversion of

[*] Y. Cao, Dr. L. Gabrielli, Dr. D. Frezzato, Prof. Dr. L. J. Prins
Department of Chemical Sciences, University of Padova
Via Marzolo 1, 35131 Padova (Italy)
E-mail: leonard.prins@unipd.it

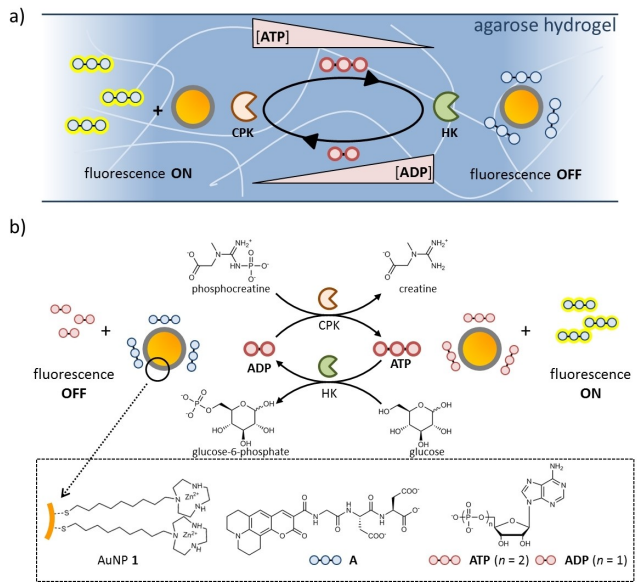

Figure 1. a) Local enzyme activity in a hydrogel results in the formation of ATP- and ADP-concentration gradients. Fluorescence patterns emerge because the displacement of probe **A** from AuNP **1** depends on the local concentrations of ATP and ADP. b) Chemically fueled cycle mediated by the enzymes creatine kinase and hexokinase that interconvert ATP and ADP. The concentrations of ATP and ADP affect the equilibrium between AuNP **1** and fluorogenic probe **A**. At high ATP concentrations, probe **A** is displaced from AuNP **1** and a high fluorescence intensity is observed. ADP is a less competitive binder and **A** is partially bound to AuNP **1** causing fluorescence quenching.

ATP into ADP the concentration-profile shifts back to the surface-bound quenched equilibrium state.

Results and Discussion

For the purpose of developing a macroscopic non-equilibrium state, chemical processes are needed that can dynamically regulate the ATP-concentration in the system.[32–36] To achieve this, we relied on chemistry previously exploited by the groups of George[37] and Hermans[38] to control dissipative self-assembly processes (Figure 1a). The ATP-concentration is regulated by two enzymatic processes. Formation of ATP occurs through the creatine kinase (CPK)-mediated transfer of the phosphate-group from phosphocreatine (PCr) to ADP. On the other hand, ATP is converted into ADP through the hexokinase (HK)-mediated transfer of the γ-phosphate from ATP to glucose. In this minimal reaction network, PCr is the reagent with high chemical potential that drives the reaction cycle and is therefore considered the fuel. Previous studies have shown that these enzymes can operate in the same solution allowing therefore the installment of a dissipative cycle in which the addition of PCr to a solution of ADP rapidly fuels the formation of ATP which is then gradually broken down again to ADP leaving glucose-6-phosphate as waste product.[37]

After an initial verification that the phosphate-containing compounds PCr and glucose-6-phosphate involved in the reaction cycle do not compete with **A** for binding to AuNP **1** (Figure S1), we verified the compatibility of both enzymes with probe displacement. In a first experiment, HK was added to a solution containing AuNP **1**, probe **A**, ATP and glucose (Figure 2a). Immediately upon addition, the fluorescence intensity started to decrease because of the conversion ATP→ADP and the consequent capture of **A** on AuNP **1**. After around 50 minutes a plateau was reached at a fluorescence intensity corresponding to a full conversion of ATP into ADP. Indeed, an analogous experiment using a mixture containing ADP and PCr started from the same fluorescent intensity (Figure 2b). Addition of CPK to this solution resulted in an immediate increase in fluorescence intensity because of ADP→ATP conversion and displacement of **A** from AuNP **1** (Figure 2b). A constant value was reached after around 100 mins corresponding to the value expected for a full conversion of ADP into ATP, *c.f.* the initial fluorescence intensity (FI) observed in the previous experiment. Extensive additional studies were carried out to investigate the response of the system towards different concentrations of reactants and enzymes (Figure S4 and S5). Under optimized conditions we carried out a final solution experiment to demonstrate that the addition of small amounts of PCr can fuel a dissipative ADP→ATP→ADP cycle in which **A** is transiently displaced from AuNP **1**. Addition of PCr to a solution containing AuNP **1**, probe **A**, ADP, glucose and both enzymes CPK and HK resulted in a

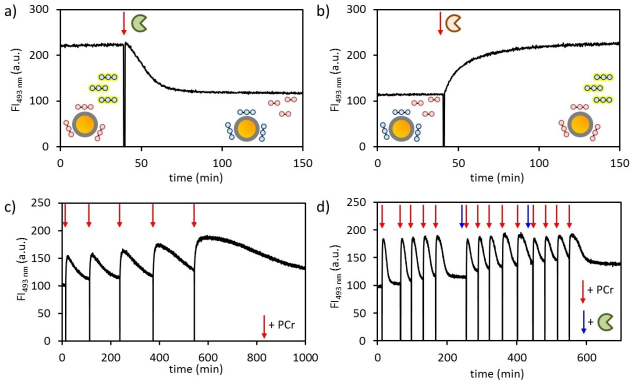

Figure 2. a) Changes in the fluorescence intensity at 493 nm upon the addition of HK to a solution containing AuNP **1**, **A**, ATP and glucose. b) Changes in the fluorescence intensity at 493 nm upon the addition of CPK to a solution containing AuNP **1**, **A**, ADP and PCr. c) Changes in the fluorescence intensity at 493 nm upon the addition of batches (10 μl) of PCr (50 μM, red arrows) to a solution containing AuNP **1**, **A**, ADP, glucose, and the enzymes HK and CPK. d) Changes in the fluorescence intensity at 493 nm upon the addition of batches of PCr (50 μM, red arrows) and HK (0.5 U ml^{-1}, blue arrows) to a solution containing AuNP **1**, **A**, ADP, glucose, and the enzymes HK and CPK. Experimental conditions: [AuNP] = 10 μM, [Zn^{2+}] = 100 μM, [**A**] = 3.5 μM, and, where applicable, [ADP] = [ATP] = 10 μM, [glucose] = 2 mM, [PCr] = 50 μM, [HK] = 0.5 U ml^{-1}, [CPK] = 0.6 U ml^{-1} (b), 2 U ml^{-1} (c) or 12 U ml^{-1} (d). All aqueous solutions were buffered with HEPES (10 mM) at pH 7.0. Instrument settings: λ_{ex} = 450 nm, λ_{em} = 493 nm, slit = 2.5/5.

rapid increase in fluorescence intensity because of the formation of ATP, but soon after the intensity dropped again to the initial level indicating that the system had returned to the quenched ADP-state (Figure 2c). The transient displacement of **A** could be repeated 5 times by adding new batches of PCr, but we noted that over time the return rate to the ADP-state slowed down indicating that HK gradually lost activity over time (Figure S6). Indeed, regular additions of fresh batches of HK (each 180 minutes) to the solution allowed up to 14 regular dissipative cycles (Figure 2d). Although the limited stability of HK is a disadvantage for the long-term operation of this kind of dissipative systems, we will later use it to our advantage to show that changes in the enzyme activity over time gives rise to interesting macroscopic behavior.

With a fuel-responsive system in hand, we then turned our attention to the first prerequisite for developing a sustained ATP-concentration gradient. This regarded the necessity to produce and consume ATP with spatial control. Recently, we have shown that a hydrogel is an attractive matrix for adding a spatial dimension to supramolecular processes.[39,40] The presence of a polymer network blocks mass transport by convection and leaves diffusion as the principal mechanism for mass transport. Because diffusion strongly depends on size, the mass transport of small molecules (like **A**, ATP/ADP, PCr, etc.) occurs on a significantly faster time scale compared to large structures (AuNP **1**, enzymes). For example, ATP ($D = 3.54 \times 10^{-6}$ cm^2 s^{-1})[41] takes around 1.5 hours to travel, on average, a distance of 2 mm along a given direction, whereas AuNP **1** ($D = 5.73 \times 10^{-7}$ cm^2 s^{-1})[39] takes around 10 hours. For the current system this difference is of relevance in two processes. First, the slow diffusion of enzyme compared to the substrates (ATP and ADP) implies that local activation of enzyme will install a concentration gradient for substrate and product. Second, the difference in diffusion rate between free and AuNP-bound **A** causes a concentration gradient of free **A** when the equilibrium between **A** and AuNP **1** is locally perturbed.

We first focused our attention on the verification of the activity of HK in hydrogel by preparing in six-well microtiter plates ($d_{well} = 3.5$ cm) agarose gels containing AuNP **1**, **A**, and the substrates for HK, i.e. ATP and glucose (Figure 3a). After stabilization of the gel, a tiny volume (1 µl) of a concentrated stock solution of enzyme (50 U ml^{-1}) was injected in the center of the gel and the fluorescence intensity of the gel was measured with spatial control using multispot-analysis for prolonged times (12 hours). The recorded data points were grouped in concentric circles with increasing distance from the injection point (positions 1–7; see Figure S7). Injection of HK resulted in an immediate decrease in fluorescence intensity in the central position 1 consistent with the conversion of ATP into ADP and the concomitant capture of probe **A** by AuNP **1** (Figure 3b+f).

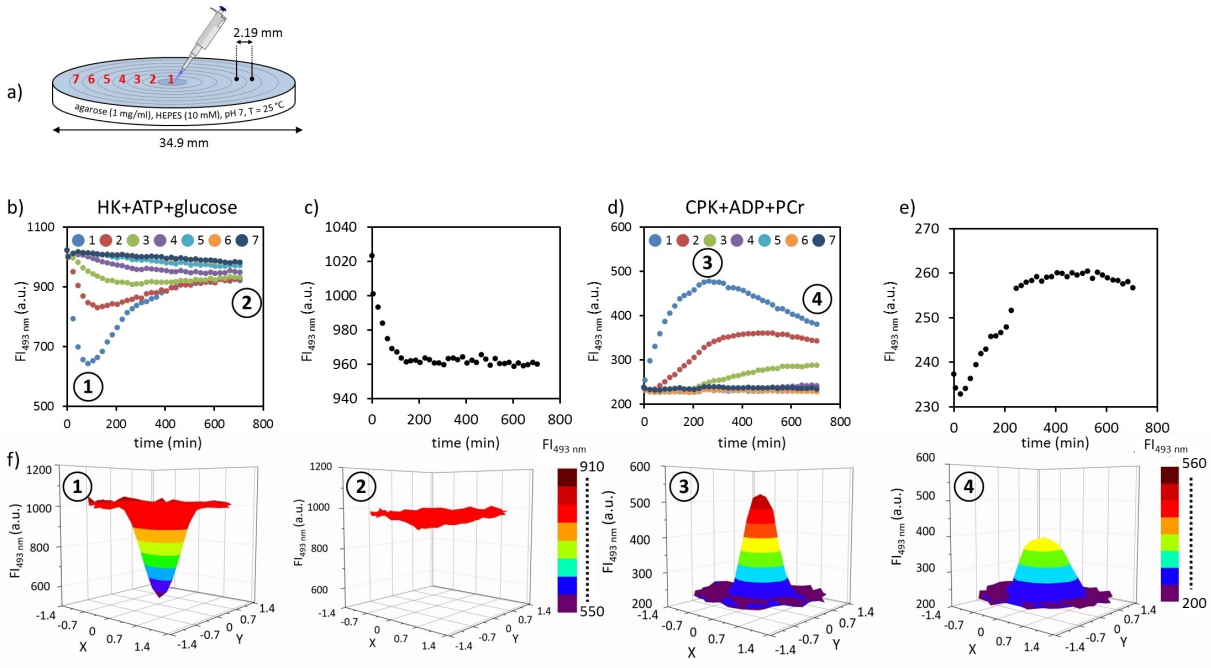

Figure 3. a) Geometrical representation of the gels used in this work indicating dimensions and the concentric circles surrounding the injection point that were used to group data points. b) Changes in the fluorescence intensity at 493 nm over time for positions 1–7 upon the injection of HK at the center of the gel. c) Changes in the overall fluorescence intensity in the gel over time calculated as the average of all data points. d) Changes in the fluorescence intensity at 493 nm over time for positions 1–7 upon the injection of CPK at the center of the gel. e) Changes in the overall fluorescence intensity in the gel over time calculated as the average of all data points. f) 3D Plots of the fluorescence intensity in the gels corresponding to the time points 1–4 indicated in Figures 3b+d. Experimental conditions: [AuNP] = 25 µM, [Zn^{2+}] = 100 µM, [**A**] = 3.5 µM, and, for 3b+c, [ATP] = 10 µM, [glucose] = 2 mM, $[HK]_{stock}$ = 50 U ml^{-1}, for 3c+d, [ADP] = 10 µM, [PCr] = 50 µM, $[CPK]_{stock}$ = 50 U ml^{-1}. Agarose gels (1 mg ml^{-1}) were buffered at pH 7.0 with HEPES (10 mM), T = 25 °C. Instrument settings: λ_{ex} = 450 nm, λ_{em} = 493 nm.

The fluorescence intensity in position 1 reached a minimum after around 100 minutes after which it gradually increased again. In time also the fluorescence intensity in other parts of the gel decreased indicating the occurrence of diffusion processes in the gel. After around 10 hours almost the same fluorescence intensity was measured all over the gel indicating that free **A** was homogeneously distributed in the gel. The duration of enzyme activity could be determined from a plot of the overall fluorescence intensity in the gel as a function of time (Figure 3c). If enzyme activity ceases, ADP is no longer produced, and no further **A** is captured on AuNP **1**. It was observed that this occurred after around 100 minutes. Evidence that reaching the plateau level was caused by a loss of HK enzyme activity was obtained by re-injecting a fresh batch of HK in position 1, which caused a further decrease in fluorescence intensity in the gel (Figure S9).

In a similar manner the activity of CPK in the hydrogel was verified. In this case, the hydrogel contained ADP and PCr in addition to AuNP **1** and **A**. The kinetic profiles of fluorescence intensity were similar as those obtained for HK, with the obvious difference that in this experiment an increase in fluorescence intensity was observed because of the production of the high-affinity binder ATP (Figure 3d+f). The observation that the overall fluorescence intensity in the gel reached a plateau level after around 300 minutes, instead of the 100 minutes observed for HK, indicated a prolonged activity of CPK compared to HK (Figure 3e).

It is of importance to note that experimentally we can only detect the concentration of free **A**, which implies that information regarding the diffusion of ATP and ADP must be inferred indirectly. For example, the decrease in fluorescence intensity in position 2—flanking position 1—upon the injection of HK can originate either from a diffusion of **A** to position 1, a capture of **A** by AuNP **1** caused by the diffusion of ADP to position 2, or both. Evidence for the diffusion of ADP was obtained from a control experiment using a gel with the same components, but containing also PCr to permit conversion of ADP into ATP. HK was injected as before, but, in addition, also the enzyme CPK was simultaneously injected at a 0.5 cm distance from HK (Figure 4a). Injection of HK in position 1 caused a similar decrease in fluorescence intensity as before, affecting first position 1 and subsequently also the neighbouring positions (Figure 4b). However, after around 150 minutes a peak in fluorescence intensity started to appear at the position where CPK was injected and this peak resisted in time (the 3D plot at 365 minutes is shown in Figure 4c). The appearance of this peak indicates that ATP is locally formed, which unequivocally demonstrates that ADP produced in position 1 had diffused to the location where CPK was injected. Likewise, a control experiment using an ADP-gel in which HK was co-injected at a small distance from CPK revealed the decrease in fluorescence intensity at the HK injection point after around 100 minutes, which confirmed that locally produced ATP had diffused through the gel (Figure S10).

Having established that both the activation and deactivation steps of the dissipative cycle function in hydrogel, we then implemented the dual enzyme system with the aim of developing persistent ATP-concentration gradients sustained by the consumption of PCr (Figure 1a). Hydrogels were prepared containing AuNP **1**, **A**, PCr and glucose and an equimolar amount of ATP and ADP. The chemical fuel PCr (50 μM) that drives the dissipative cycle was added at a 10-fold higher concentration compared to ATP and ADP (5 μM each). Both CPK and HK were injected in the gel separated by a distance of 0.5 cm and the fluorescence intensity of the gel was followed over time (Figure 5a). 3D Plots of the fluorescence intensity clearly reveal the immediate formation of a maximum centered around the CPK-injection point and a minimum centered around the HK-injection point resulting respectively from a local increase and decrease in ATP (Figure 5b). These macroscopic features persisted for several hours with the negative peak fading out earlier. Based on the experiments described above we attributed this to a loss of HK activity over time. After 10 hours a rather homogeneous intensity was observed at an average value that was higher than the initial intensity.

To gain more insight in the instalment and evolution of ATP-concentration gradients in the system we developed a reaction-diffusion model that takes into consideration all relevant kinetic processes occurring in the system. A detailed description of the model and the physical inputs used to carry out the simulations is provided in the Supporting Information. In short, the model treats the hydrogel as a 2D grid composed of multiple square cells. Concentrations in each cell evolve in time as a result of supramolecular exchange processes occurring on AuNP **1** (involving species **A**, ATP, and ADP), chemical reactions (ATP- and ADP-formation are treated as 2nd order reactions with the respective reactants PCr and glucose) and diffusion (exchange between cells of all species except for AuNP **1**, molecules bound to AuNP **1**, and enzymes HK and CPK).

We simulated all three experiments described above (Figures 3b+3d, Figure 5a), but here we discuss in detail just the results of the last most important experiment in which a pseudo-stationary non-equilibrium state is generated with a persistent ATP-concentration gradient. Initial concentrations were set to 5 μM for ATP and ADP each and enzyme injection was simulated by allowing ATP- and ADP-forming reactions just in two points of the matrix separated by 0.5 cm, just as in the experiment. Analysis of the concentration of free **A** in the matrix over time—which corresponds to the parameter that can be experimentally detected—showed that the simulation provided a description in agreement with the experimental observation (Figure 5c). Almost instantly, a maximum and minimum appear at the cells where enzyme activity of CPK and HK, respectively, are simulated and these signatures broaden over time. The simulation also reproduces faithfully the experimentally observed evolution of the signal, leading eventually to a homogeneous distribution of free **A** in the system. The coherence between the simulated and experimental data shows that the model qualitatively describes what happens in the gel. We therefore analysed the evolution of ATP- and ADP-concentrations in the simulations as these cannot be directly detected experimentally. As expected, local changes

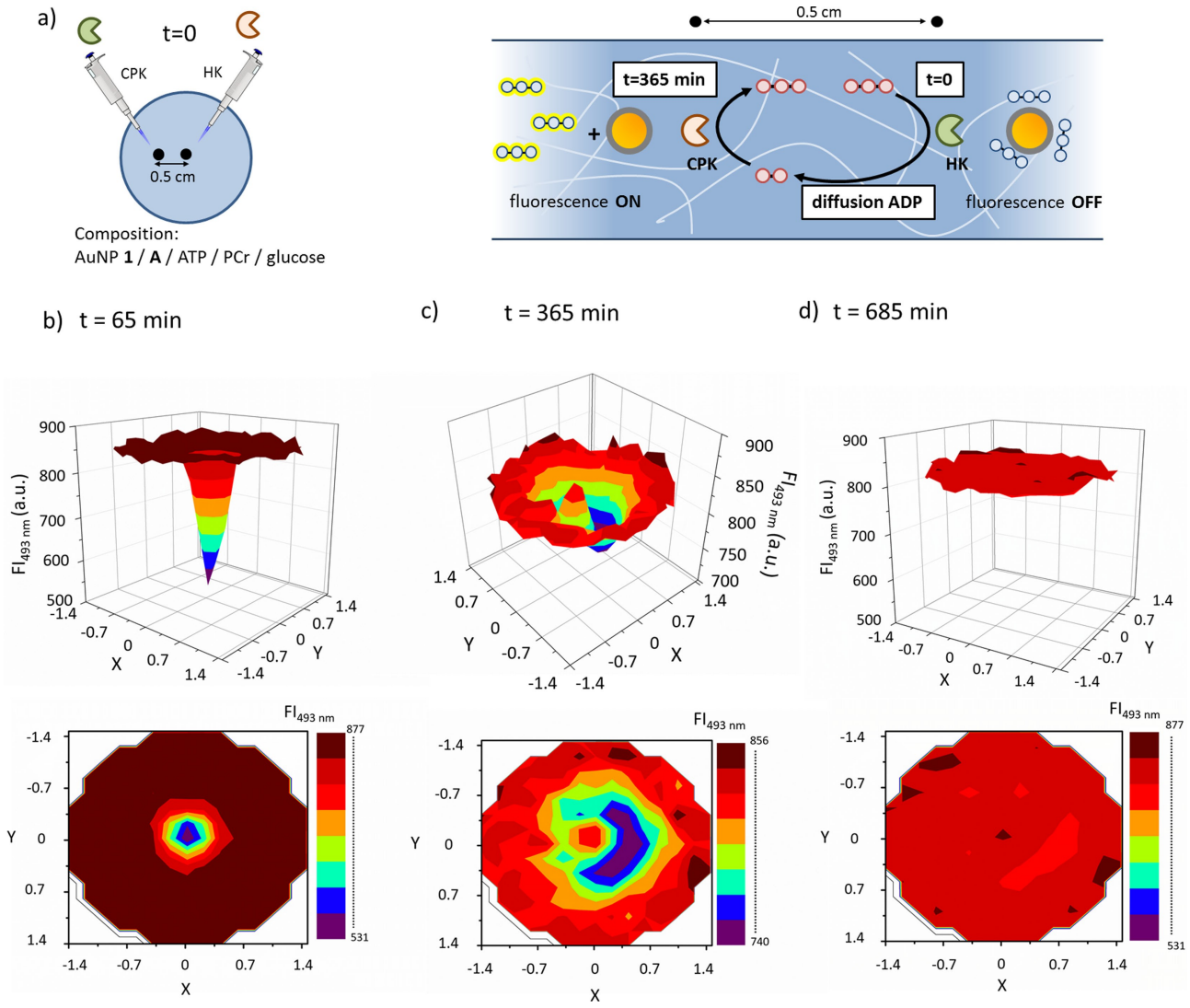

Figure 4. a) Injection of both CPK and HK in a gel containing ATP, PCr, and glucose results in the localized production of ADP at the HK-injection point. Diffusion of ADP through the gel causes a capture of **A** on AuNP **1** with concomitant decrease in fluorescence intensity. When ADP arrives at the CPK injection point, it reacts with PCr to form ATP. The locally enhanced concentration of ATP causes a local higher fluorescence intensity. b) 3D and 2D plots of the fluorescence intensity in the gel at $t=65$ min. c) 3D and 2D plots of the fluorescence intensity in the gel at $t=365$ min. d) 3D and 2D plots of the fluorescence intensity in the gel at $t=685$ min. Experimental conditions: [AuNP] = 25 μM, $[Zn^{2+}]=100$ μM, [**A**] = 3.5 μM, [ATP] = 10 μM, [PCr] = 50 μM, [glucose] = 2 mM, $[HK]_{stock}=100\ U\,ml^{-1}$, $[CPK]_{stock}=100\ U\,ml^{-1}$. Agarose gel (1 mg ml^{-1}) was buffered at pH 7.0 with HEPES (10 mM), $T=25\,^{\circ}C$. Instrument settings: $\lambda_{ex}=450$ nm, $\lambda_{em}=493$ nm.

in ATP and ADP concentration occur immediately as a result of enzyme reactivity. A main difference with the evolution of the concentration of **A** is that the local maxima and minima for ATP and ADP persist for much longer times (Figure 5d + 5e). Indeed, the fact that the ATP- and ADP-concentrations gradients in the simulations remain unaltered over an extended period of time indicates that the system resides in a (pseudo-) stationary state (Figure S11). This state is not visible from the concentration gradient of free **A** in the system because at the (pseudo-)stationary state no driving force exists to maintain it. Figure 5f shows the contour plot of the ATP landscape for the system under (pseudo-) stationary steady state conditions ($t=10^7$ s). The vectors associated with the ATP time-dependent diffusion current are perpendicular to the contour lines and illustrate that at the (pseudo-) stationary state ATP and ADP predominantly diffuse in a cyclic manner between the CPK and HK sites (Figure 1a).

We stress that the model is based on simplifying assumptions. In particular, nanoparticles and enzyme molecules are treated as immobile in the gel matrix. While the diffusion of the nanoparticles likely plays a negligible role (since their initial distribution is already isotropic and because the binding/unbinding events are fast), the diffusion of the enzymes is expected to cause a quicker broadening of the concentration peaks and to affect the duration of the (pseudo-) stationary state. The present basic model, however, enables us to shed light on the main features. In

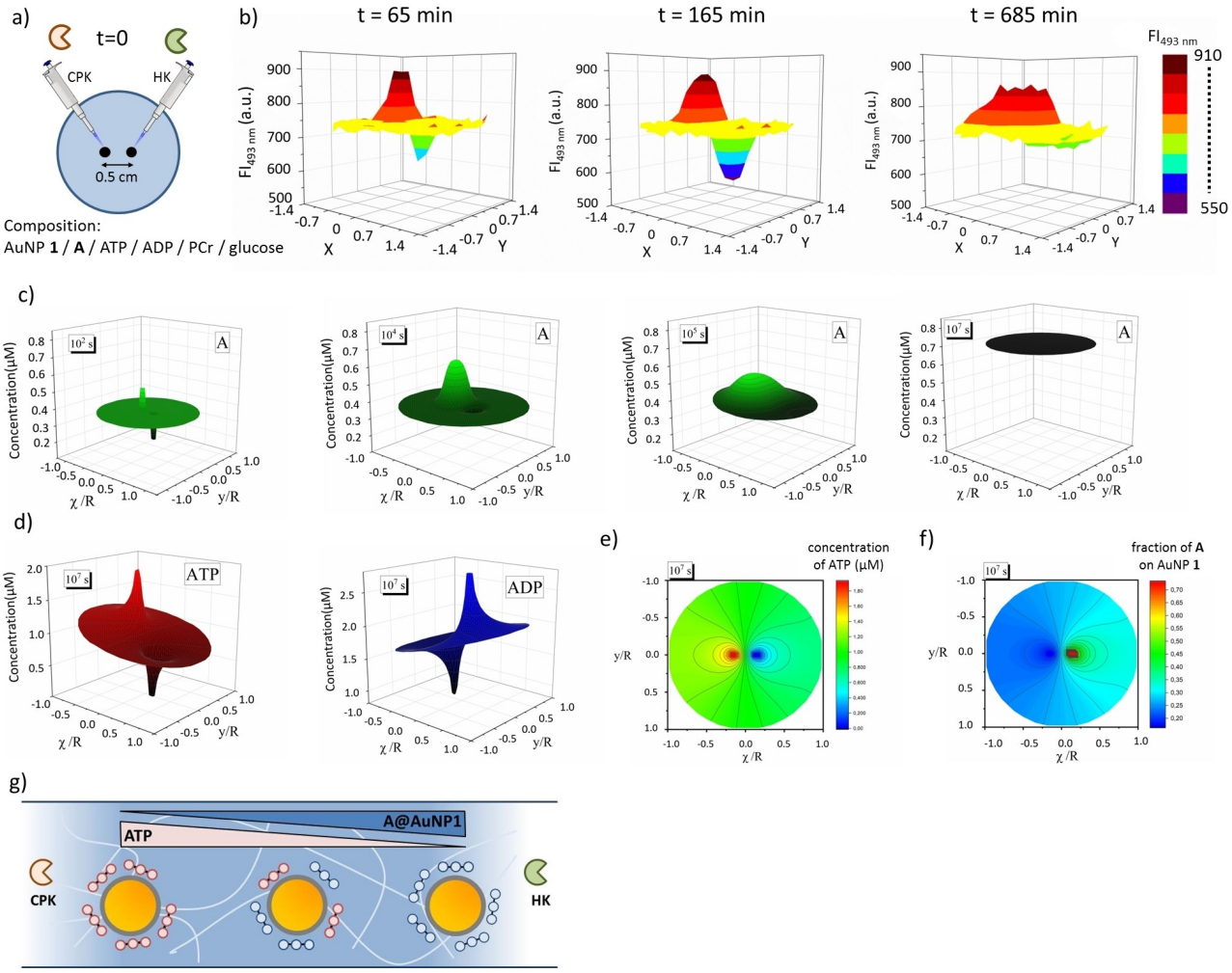

Figure 5. a) Schematic overview of the gel that is maintained in a (pseudo-) stationary non-equilibrium state through the local activity of the enzymes CPK and HK. b) 3D Profiles of the fluorescence intensity at 493 nm at three different times ($t=65$, 165 and 685 mins) after injection of CPK and HK at the positions indicated in Figure 5a. c) Calculated 3D Profiles of the concentration of **A** at three different times ($t=10^2$, 10^4, 10^5 and 10^7 s). d) Calculated 3D Profiles of the concentrations of ATP and ADP at the (pseudo-) stationary state ($t=10^7$ s). e) Calculated contour plot of the ATP concentration landscape at $t=10^7$ s. f) Calculated 2D profile of the fraction of **A** bound to AuNP **1** at $t=10^7$ s. g) Schematic representation showing how the surface composition of AuNP **1** depends on the ATP-concentration gradient.

particular, the simulations permit an insight in an important feature of the system, which is the surface composition of AuNP **1**. The competition between ATP, ADP and probe **A** for binding to the cationic monolayer of AuNP **1** implies that the surface composition is coupled to the macroscopic ATP and ADP concentration gradients. This coupling is confirmed by a 2D plot of the fraction of **A** on the surface of AuNP **1**, which shows enrichment in the ADP-rich areas and diminution in the areas rich in ATP (Figure 5g). It is of relevance to note, that the surface composition on AuNP **1** remains biased as long as ATP- and ADP-conversion takes place. The possibility to regulate the surface composition in function of energy consumption offers new possibilities to control the properties of AuNP **1** regarding multivalency and catalysis.[42]

The local injection of enzymes in a hydrogel matrix offers precise control over the position where chemical reactions are activated and therefore offers a straightforward way to install complex ATP-concentration gradients in a controlled manner. To illustrate the versatility of the approach and to illustrate how the dynamics originating from coupling a supramolecular process to a reaction-diffusion system can give rise to intricate fluorescence patterns that evolve over time, we carried out an experiment in which the enzymes HK and CPK were injected at three different locations (Figure 6a). The initial gel contained AuNP **1**, **A**, PCr, glucose and ATP. The presence of just ATP implies that **A** is mostly present in the free form and not bound to AuNP. HK was injected in the center of the gel and CPK at two positions distanced from the center by 0.5 cm. An initial decrease in fluorescence intensity was observed at the HK injection point caused by the conversion of ATP into ADP, which gradually involved also neigbouring positions (Figure 6b, $t=165$ min). Similar to the HK-experiment described above, after around 3 hours the fluorescence intensity started to increase again, but, surpris-

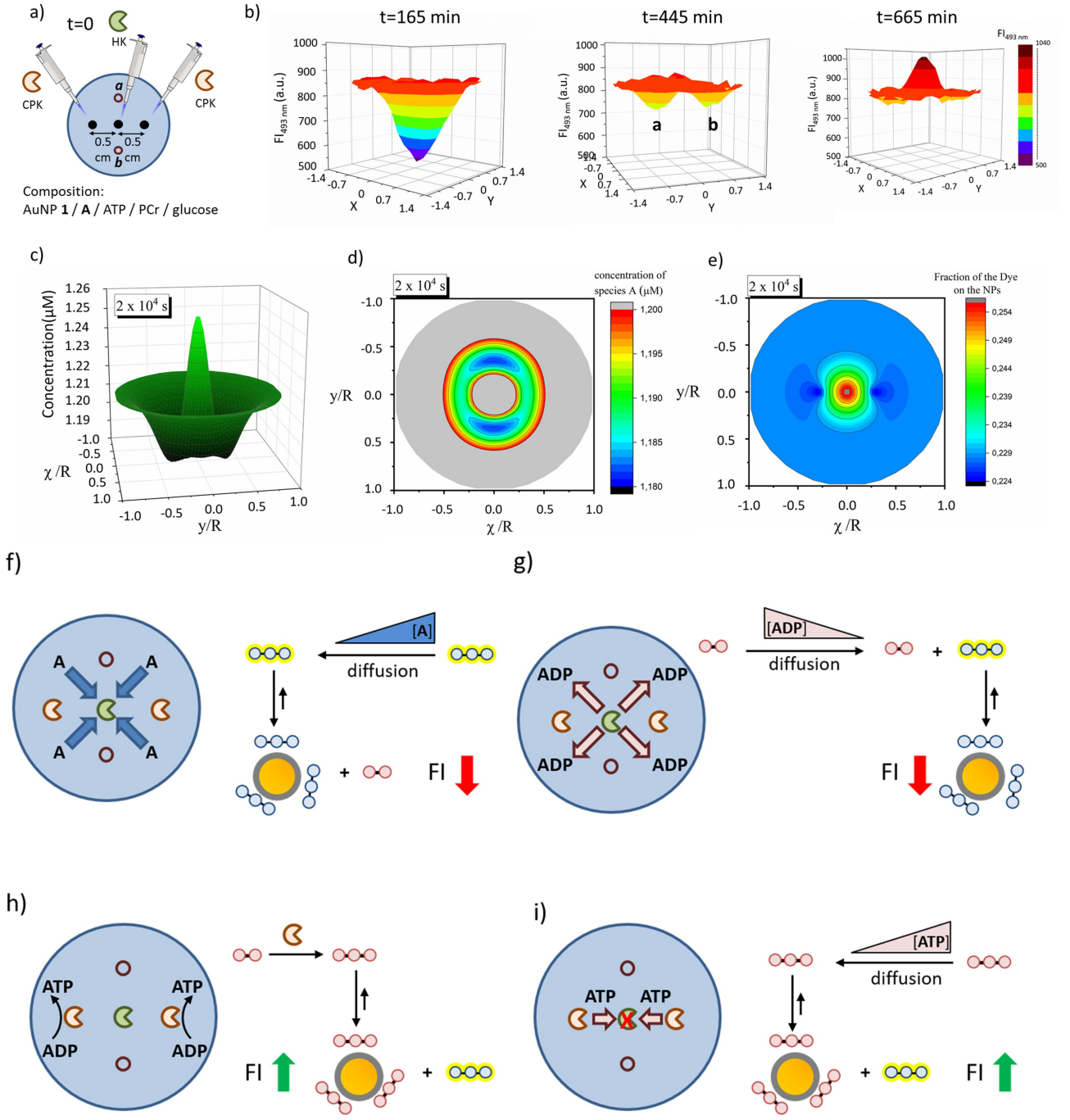

Figure 6. a) Schematic overview of the gel that was subjected to the injection of HK (center) and CPK (two injections at 0.5 cm distance from the center). b) 3D Profiles of the fluorescence intensity at 493 nm at three different times ($t=165$, 445 and 665 mins) after injection of CPK and HK at the positions indicated in Figure 6a. c) Calculated 3D and 2D profiles of the concentration of **A** at $t=2\times10^4$ s after deactivation of HK at 5×10^3 s (see Supporting Information for details). d) Schematic representation that shows how the conversion of ATP into ADP causes the accumulation of **A** during the initial stages of the experiment. e) Diffusion of ADP from the center to other parts of the gel causes a decrease in fluorescence intensity in the gel. f) Back-conversion of ADP into ATP at the CPK-injection points leads to a local increase in fluorescence intensity, which indirectly causes the formation of two minima in fluorescence intensity at positions **a** and **b**. g) ATP produced by CPK diffuses preferentially back to the center and displaces **A** from AuNP **1** that had accumulated during the initial stages. h) Calculated 2D profile of the fraction of **A** bound to AuNP **1** at $t=2\times10^4$ s.

ingly, in time a 3D profile emerged with a maximum at the HK-injection point and two minima at positions ***a*** and ***b*** from the center (Figure 6b, $t=665$ min). To understand the emergence and evolution of the fluorescent pattern a kinetic model was developed that was able to reproduce qualitatively the pattern evolution (Figure 6c). Simulations showed that conversion of ATP into ADP in the central position results in a capture of **A** on AuNP **1** which installs a flow of

A towards the center (Figure 6d). The result of this first phase is therefore an accumulation of **A** on AuNP **1** at the HK-injection point. At the same time, conversion of ATP into ADP in position 1 causes a gradual increase in ADP concentration—and decrease in ATP concentration—in the gel starting from the center. Diffusion of ADP gradually causes a decrease in fluorescence intensity at increasing distances from the center (Figure 6e). However, ADP diffusing in the direction of CPK is re-converted into ATP causing the fluorescence intensity to increase, but just at the CPK-positions (Figure 6f). Since ATP is not regenerated at positions **a** and **b**, this explains the presence of minima in fluorescence intensity at those positions.

Yet, the formation of the maximum at the center—which is surprising considering that it is the position where ADP is formed—turned out to be harder to explain. The ATP produced at the CPK-sites diffuses preferentially back to the center, because the concentration gradient is steeper in that direction. However, simulations show that this is not sufficient to explain the observed maximum. The fluorescence intensity in the center would just gradually increase yielding eventually a homogeneous fluorescence intensity all over the gel, but without a maximum at the center. Simulations showed that the observed experimental profile is a result of the loss of HK activity over time. In the absence of HK activity, ATP that diffuses back to the center is no longer converted in ADP and displaces **A** from AuNP **1** that had accumulated during the initial phase (Figure 6g). This displacement causes the observed 'burst' in fluorescence intensity at the center. So, although in this system the peculiar formation and evolution of the pattern results from a 'fortunate' spontaneous deactivation of HK, it provides a glimpse of the complex patterns that can evolve in a macroscopic system in which catalytic activity can be locally activated *and* deactivated (for example through the addition of inhibitors). Finally, an analysis of the fraction of **A** bound to AuNP **1** demonstrates that at the stationary non-equilibrium state the surface composition of AuNP **1** depends on the spatial position in the gel (Figure 6h). This illustrates that local chemical upregulation provides a tool to create patterns of AuNP **1** characterized by different surface compositions.

Conclusion

We have developed an approach that permits the controlled formation of macroscopic ATP-concentration gradients that are sustained in time by the consumption of a chemical fuel. The concentration gradients persist as long as chemical fuel is present in the system. At the (pseudo-) stationary non-equilibrium state ATP and ADP diffuse preferentially between the sites where ATP is produced and consumed, respectively. An important element is the use of a hydrogel as an inert matrix as it permits the difference in diffusion rate between large and small objects to be used to activate chemical processes with spatial control. The supramolecular system composed of AuNP **1** and **A** is used as a model system to demonstrate that the combination of chemical reactivity, supramolecular processes and diffusion can give rise to the formation of macroscopic patterns that dynamically evolve over time.

An attractive feature of the approach is that it permits the rational formation of complex concentration gradients through multipoint injections of enzymes. Future studies will be aimed at understanding how the initial conditions (injection points, type of loads, loads, etc.), boundaries (shape and dimension of the wells) and kinetic parameters (enzymatic rates, diffusion coefficients) affect the concentration profiles. We are convinced that this kind of systems may find use as synthetic models for understanding how concentration gradients affect biological processes in the cell.

Acknowledgements

This work was financially supported by the China Science Council (Y. C.), the Italian Ministry of Education and Research (L.J.P., grant 2017E44 A9P) and the University of Padova (L.J.P., P-DiSC #CASA- BIRD2022-UNIPD).

Conflict of Interest

The authors declare no conflict of interest.

Data Availability Statement

The data that support the findings of this study are available from the corresponding author upon reasonable request.

Keywords: Chemical Fuel · Concentration Gradient · Hydrogel · Non-Equilibrium · Self-Assembly

[1] E. Schrödinger, *What Is Life? The Physical Aspect of the Living Cell*, Cambridge Univ Press, Cambridge, UK, **1944**.
[2] R. D. Astumian, *Biophys. J.* **2010**, *98*, 2401–2409.
[3] J. K. Lanyi, A. Pohorille, *Trends Biotechnol.* **2001**, *19*, 140–144.
[4] D. C. Gadsby, *Nat. Rev. Mol. Cell Biol.* **2009**, *10*, 344–352.
[5] P. Bastiaens, M. Caudron, P. Niethammer, E. Karsenti, *Trends Cell Biol.* **2006**, *16*, 125–134.
[6] F. M. Harold, *Microbiol. Mol. Biol. Rev.* **2005**, *69*, 544–564.
[7] B. A. Grzybowski, W. T. S. Huck, *Nat. Nanotechnol.* **2016**, *11*, 585–592.
[8] R. Merindol, A. Walther, *Chem. Soc. Rev.* **2017**, *46*, 5588–5619.
[9] S. A. P. van Rossum, M. Tena-Solsona, J. H. van Esch, R. Eelkema, J. Boekhoven, *Chem. Soc. Rev.* **2017**, *46*, 5519–5535.
[10] Y. Feng, M. Ovalle, J. S. W. Seale, C. K. Lee, D. J. Kim, R. D. Astumian, J. F. Stoddart, *J. Am. Chem. Soc.* **2021**, *143*, 5569–5591.
[11] I. Aprahamian, *ACS Cent. Sci.* **2020**, *6*, 347–358.
[12] S. Borsley, D. A. Leigh, B. M. W. Roberts, *Nat. Chem.* **2022**, *14*, 728–738.
[13] K. Mo, Y. Zhang, Z. Dong, Y. Yang, X. Ma, B. L. Feringa, D. Zhao, *Nature* **2022**, *609*, 293–298.
[14] K. Gentile, A. Somasundar, A. Bhide, A. Sen, *Chem* **2020**, *6*, 2174–2185.

[15] S. Ghosh, A. Somasundar, A. Sen, *Annu. Rev. Condens. Matter Phys.* **2021**, *12*, 177–200.
[16] P. A. Korevaar, C. N. Kaplan, A. Grinthal, R. M. Rust, J. Aizenberg, *Nat. Commun.* **2020**, *11*, 386.
[17] A. van der Weijden, M. Winkens, S. M. C. Schoenmakers, W. T. S. Huck, P. A. Korevaar, *Nat. Commun.* **2020**, *11*, 4800.
[18] I. R. Epstein, B. Xu, *Nat. Nanotechnol.* **2016**, *11*, 312–319.
[19] A.-D. C. Nguindjel, P. J. de Visser, M. Winkens, P. A. Korevaar, *Phys. Chem. Chem. Phys.* **2022**, *24*, 23980–24001.
[20] P. R. A. Chivers, D. K. Smith, *Nat. Rev. Mater.* **2019**, *4*, 463–478.
[21] H. S. Cooke, L. Schlichter, C. C. Piras, D. K. Smith, *Chem. Sci.* **2021**, *12*, 12156–12164.
[22] L. Schlichter, C. C. Piras, D. K. Smith, *Chem. Sci.* **2021**, *12*, 4162–4172.
[23] J. Raeburn, B. Alston, J. Kroeger, T. O. McDonald, J. R. Howse, P. J. Cameron, D. J. Adams, *Mater. Horiz.* **2014**, *1*, 241–246.
[24] S. O. Krabbenborg, J. Veerbeek, J. Huskens, *Chem. Eur. J.* **2015**, *21*, 9638–9644.
[25] I. Maity, C. Sharma, F. Lossada, A. Walther, *Angew. Chem. Int. Ed.* **2021**, *60*, 22537–22546; *Angew. Chem.* **2021**, *133*, 22711–22720.
[26] X. Fan, A. Walther, *Angew. Chem. Int. Ed.* **2021**, *60*, 3619–3624; *Angew. Chem.* **2021**, *133*, 3663–3668.
[27] N. Priyanka, E. Shandilya, S. K. Brar, R. R. Mahato, S. Maiti, *Chem. Sci.* **2022**, *13*, 274–282.
[28] R. R. Mahato, N. Priyanka, E. Shandilya, S. Maiti, *Chem. Sci.* **2022**, *13*, 8557–8566.
[29] L. J. Prins, *Acc. Chem. Res.* **2015**, *48*, 1920–1928.
[30] R. Bonomi, A. Cazzolaro, A. Sansone, P. Scrimin, L. J. Prins, *Angew. Chem. Int. Ed.* **2011**, *50*, 2307–2312; *Angew. Chem.* **2011**, *123*, 2355–2360.
[31] C. Pezzato, L. J. Prins, *Nat. Commun.* **2015**, *6*, 7790.
[32] A. Mishra, S. Dhiman, S. J. George, *Angew. Chem. Int. Ed.* **2021**, *60*, 2740–2756; *Angew. Chem.* **2021**, *133*, 2772–2788.
[33] J. Deng, A. Walther, *Adv. Mater.* **2020**, *32*, 2002629.
[34] J. Deng, A. Walther, *Nat. Commun.* **2020**, *11*, 3658.
[35] L. Heinen, A. Walther, *Sci. Adv.* **2019**, *5*, eaaw0590.
[36] M. Kumar, P. Brocorens, C. Tonnelé, D. Beljonne, M. Surin, S. J. George, *Nat. Commun.* **2015**, *6*, 5793.
[37] S. Dhiman, A. Jain, S. J. George, *Angew. Chem. Int. Ed.* **2017**, *56*, 1329–1333; *Angew. Chem.* **2017**, *129*, 1349–1353.
[38] A. Sorrenti, J. Leira-Iglesias, A. Sato, T. M. Hermans, *Nat. Commun.* **2017**, *8*, 15899.
[39] R. Chen, S. Neri, L. J. Prins, *Nat. Nanotechnol.* **2020**, *15*, 868–874.
[40] R. Chen, K. Das, M. A. Cardona, L. Gabrielli, L. J. Prins, *J. Am. Chem. Soc.* **2022**, *144*, 2010–2018.
[41] M. J. Hubley, T. S. Moerland, R. C. Rosanske, *NMR Biomed.* **1995**, *8*, 72–78.
[42] L. J. Prins, F. Mancin, P. Scrimin, *Curr. Org. Chem.* **2009**, *13*, 1050–1064.

Manuscript received: October 19, 2022
Accepted manuscript online: November 24, 2022
Version of record online: December 15, 2022